SEMARAK ILMU PUBLISHING

Journal of Advanced Research in Fluid Mechanics and Thermal Sciences

Journal homepage:
https://semarakilmu.com.my/journals/index.php/fluid_mechanics_thermal_sciences/index
ISSN: 2289-7879

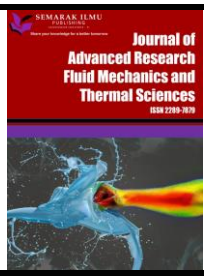

Computational Study on the Influence of Duct on The Performance of Darrieus Hydro-Turbine

Dominic Laja Munggau[1], Djamal Hissein Didane[2,*], Sami Al-Alimi[1], Yazid Abdullsameea Mohammed Saif[1], Bukhari Manshoor[2]

[1] Department of Mechanical Engineering, Faculty of Mechanical and Manufacturing Engineering, Universiti Tun Hussein Onn Malaysia, Malaysia
[2] Center for Energy and Industrial Environment Studies (CEIES), Faculty of Mechanical and Manufacturing Engineering, Universiti Tun Hussein Onn Malaysia, Malaysia

ARTICLE INFO

Article history:
Received 23 December 2022
Received in revised form 28 March 2023
Accepted 7 April 2023
Available online 22 April 2023

Keywords:
Blade design; HAWT; CFD Fluent; power coefficient; torque coefficient

ABSTRACT

Hydropower is considered one of the most reliable, inexpensive and environmentally friendly sources of renewable energies and it is predicted to play a significant role in future sustainable energy systems. The straight-blade Darrieus turbine is receiving more attention as it is simple to build at an inexpensive cost. However, Darrieus turbines still have a lower efficiency as opposed to axial turbines. Therefore, in this study, the Darrieus turbine is equipped with a duct geometry in the center in order to enhance its conversion efficiency using the computational fluid dynamics (CFD) simulation technique. A 2D simulation model with NACA 663-018 airfoil profile is developed to perform the simulation in Ansys Fluent software while using the K-ω shear stress transport (SST) as the turbulence model. The computational simulations cover a parametric study based on the variation of the rotational speeds while keeping the upstream velocity constant. The performances are evaluated in terms of power, power coefficient, torque and torque coefficient. The simulation results showed that the power coefficient and torque coefficient were found to increase with the rotational speeds with the highest efficiency at the TSR of 2 and then decrease. A similar conclusion was drawn in terms of power and torque output. However, the maximum power coefficient and torque coefficient were about 54% and 27%, respectively.

1. Introduction

Modern societies rely on energy to power modern technological achievements including manufacturing, transportation, food, medicine, and communication, as well as human civilization. During the last few decades, many corporations involved in energy production have been researching and digging into renewable energy to replace non-renewable energy. Despite efforts to reduce the use of non-renewable energy such as nuclear power, coal and fossil fuels, which are the primary contributors to climate change due to excessive carbon dioxide emissions, the world continues to fall short of the Paris Agreement's international climate goals, as well as the international goals for

* *Corresponding author.*
E-mail address: djamal@uthm.edu.my

https://doi.org/10.37934/arfmts.105.1.210219

sustainable development. As several studies suggest, it remains less than a decade to keep the global warming below 1.5°C and prevent the worst effects of climate change, according to the IPCC's 2018 Special Report on 1.5°C [1]. Nowadays, almost every complicated technical product or item that is vital part of our civilization today requires energy. As a result, electric energy has evolved into both modern life and a catalyst for technological advancement and human civilization. Unfortunately, given that most of the existing electricity comes from coal, nuclear, and other non-renewable power plants, the process of producing electricity around the world is one of the major sources of pollution. Thus, clean energy solutions are required to meet these demands and address global concerns about environmental pollution and climate change caused by the consumption of conventional resources. As a result, demand for both renewable and cost-effective sustainable energy sources has risen rapidly around the world [2].

However, although green energy resources such as wind and solar are receiving more attention today as a means to transit towards zero-energy emissions due technological development and drop of cost, hydropower technology is utilized to generate electricity in more than 160 countries across the world. It generates roughly 3,500 TWh per year, accounting for 15.8 percent of worldwide energy generation with a total installed capacity of 1060 GW [1]. Therefore, it is expected to remain a vital component of future sustainable energy systems. This is due to its low cost per kilowatt hours electricity and dependable source of renewable and ecologically friendly electricity [3]. According to Ahuja and Tatsutani [4], the demand for both renewable and cost-effective sustainable energy sources has risen rapidly around the world. Moreover, hydropower is one of the least expensive and most reliable source of renewable and environmentally friendly electricity and it is predicted to play an important role in the future, as such more research on the use of hydropower are conducted globally, particularly the hydrokinetic turbine as a sustainable energy source to replace the traditional use of fossil fuels and coals in power generation [5]. Furthermore, the mechanism of this renewable energy source uses hydrokinetic turbines that transfer the kinetic energy of the river, where they function under a potential energy differential generated by dams. Then the hydroelectric components create electricity by catching the mechanical energy of falling water and converting it to electricity through a turbine where the generator converts the mechanical energy of the turbine into electrical energy. Hydrokinetic energy can be found in rivers, streams, tidal currents and marine currents. In addition, at hydroelectric plants, built-in dams impound rivers raising the water level behind the dam and delivering the maximum possible head. As the amount of potential power generated by a volume of water is related to the working head, a high-head configuration takes less water to generate the same amount of power as a low-head setup [6].

Among the typical turbines used are the Darrieus turbines which are crossflow hydrokinetic turbines. In recent decades, hydrokinetic energy conversion has grown in popularity and the utilization of the Darrieus turbine to convert hydrokinetic energy has increased [7]. For small-scale projects, it is employed as a stand-alone unit and an array of vertical-axis turbines has been proposed for scaling up [8]. The main advantage of the Darrieus turbine with straight blades is the ease of construction which makes it very cost-effective on the other hand, has a lower power coefficient than axial turbines and a various torque output. While other types of hydro turbines are able to overcome some of the Darrieus turbine's limitations, they have a complex design that demands specialized manufacturing processes which increase the cost of the turbine [9]. Therefore, over the years, there were substantial efforts to improve the performance of Darrieus turbine rotors including both active and passive techniques using conventional experimental and simulation approaches. Among the notable active techniques are the use of counter-rotating rotors, double-stage rotors, perforated rotors, inner blades, modifications on the blade shape, etc. and the use of diffusers, a rotating deflector placed upwind the rotor, etc. as a passive method to improve the turbine rotors [10–19].

As a such, the main objective of this study is to investigate the effects of duct geometry on the performance of the Darrieus hydroturbine while hoping to further understand the importance and impact of duct geometry on the performance of Darrieus hydroturbine.

2. Mathematical formulations

2.1 Governing Equations

The governing equations involved in this study are the Navier – Stokes equations which include the mass and momentum equations, as shown in Eq. (1) and Eq. (2), respectively for incompressible turbulence flow. The performance of turbulence flow characteristics are quantified by using the two equations hybrid k-ω shear stress transport (SST) turbulence model since it is more effective compared to the k-ε model when near the wall functions are sensitive [20]. The two equations for turbulence kinetic energy, k (m^2/s^2) and specific turbulent dissipation rate, ω (s^{-1}), are shown respectively in Eq. (3) and Eq. (4).

$$\frac{\partial u_i}{\partial x_i} = 0 \tag{1}$$

$$\frac{\partial U_i}{\partial t} + U_j \frac{\partial U_i}{\partial x_j} = -\frac{1}{\rho}\frac{\partial p}{\partial x_i} + v\frac{\partial}{\partial x_j}\left(\frac{\partial u_i}{\partial x_j}\right) + \frac{\partial}{\partial x_j}\left(-u_i' u_j'\right) + x \tag{2}$$

$$\frac{\partial (k u_i)}{\partial x_j} = \frac{\partial}{\partial x_j}\left(\frac{T_k}{\rho}\frac{\partial k}{\partial x_j}\right) + P + \gamma_k \tag{3}$$

$$\frac{\partial (\omega u_i)}{\partial x_j} = \frac{\partial}{\partial x_j}\left(\frac{T_\omega}{\rho}\frac{\partial \omega}{\partial x_j}\right) + G_\omega + \gamma_k + D_\omega \tag{4}$$

2.2 Performance Parameters

In this analysis, some theoretical calculations are employed to determine the various amounts of outputs to be compared to the outcomes of the simulations. The following equations are used to calculate tip speed ratio (TSR), torque, power, power coefficient and torque coefficient, as shown respectively in Eq. (5)-Eq. (8).

$$\lambda = \frac{\omega R}{V} \tag{5}$$

where: ω is the angular speed of the turbine blade and R is the radius of the turbine

$$P = T\omega \tag{6}$$

$$C_p = \frac{P}{{}^1/_2 \rho A V^3} \tag{7}$$

where: ρ is the density of the water, A is the turbine swept area and V is the inlet velocity

$$C_T = \frac{C_p}{\lambda} \tag{8}$$

where: λ is the tip speed ratio (TSR)

3. Materials and Methods

3.1 Blade Design

In this study, the NACA 63_3-018 airfoil profile was chosen to be investigated using a 2D geometry. Following the selection of an airfoil, the calculated coordinates of the airfoil which are available in the airfoil database are rearranged and reformatted in Microsoft Excel before being transferred into the ANSYS software in order to create an airfoil model in the ANSYS DesignModeler Geometry. The rotor developed comprises three blades and diameter of the rotor and chord length are 1.6 m and 0.3 m. Table 1 below shows the geometrical specifications of the present NACA 63_3-018 turbine.

Table 1
The specification of the turbine

Parameter	Details
Number of Blades	3
Blade Profile	NACA 63_3-018
Rotor Diameter	1.6 m
Chord length	0.3 m
Solidity	0.179

3.2 Spatial Domain Discretization, Boundary Conditions and Setup

The computational domain consists of two regions. A rectangular fixed region which represents the overall calculation region and a non-fixed circular region where the rotor is set to rotate. The two regions are separated by an interface boundary condition. The streamwise distance is fifteen times the diameter of the rotor which is 24 m while sideway distance is ten time the diameter which is 16 m. The rotor was placed at 8 m away from the inlet position. Moreover, the boundary conditions are an important part of simulation process since they are utilized as flow variables to control and guide the motion of the physical model. Proper guidance of the flow of the flow will lead to a precise solution. As a result, it is critical to correctly characterize the boundary conditions of each geometry of the component during the pre-processing step, as the solution to flow issues is dependent on it. Any unassigned boundary conditions may create errors during simulations or result in erroneous findings. There are various boundary conditions in this study such as the inlet and outlet boundaries. In this study, a velocity with a stable distribution of 1.1 m/s is given to the inlet in the x-axis direction while a zero pressure is applied to the outlet boundary condition. Meanwhile, the side walls are assigned as slip wall boundary condition and the rotating blades as non-slip wall boundary condition in order to capture the shear condition and standard roughness.

Furthermore, as the quality of the mesh cells formed has a significant impact on the precision and accuracy of the flow solution, all-triangles mesh was used in this study, as shown in Figure 1. The mesh cells are concentrated around the airfoil body and the element size increases smoothly as the distance increases away from the walls. In terms of solution techniques, the pressure-velocity coupling scheme was used as the numerical schemes and algorithms of the solution.

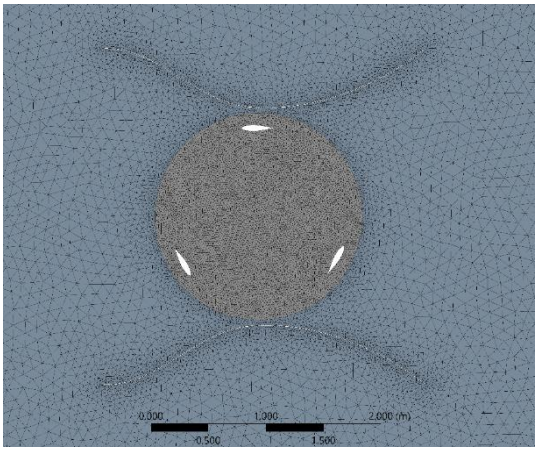

Fig. 1. Meshing of the NACA633-018 airfoil

4. Results and discussion

4.1 Model Validation

Before continuing with the simulations, one key step must be done, which is to compare the simulation findings to the results of past studies. This allows us to know if the simulation approach being used is trustworthy and accurate enough to be used for the remaining simulations. As a consequence, a validation procedure was carried out by comparing the present simulation results with the prior research conducted by Malipeddi *et al.,* [21] in order to ascertain that the present findings are closest to the previous results. The two studies are validated in terms of power coefficient for the models with duct and without duct in a TSR range between 1.6 to 3.2, as shown in Figure 2. The figure illustrates that the pattern between the present and prior research results is comparable from beginning to end, which is good and acceptable. The relative error was determined to be about 10.45 % on average.

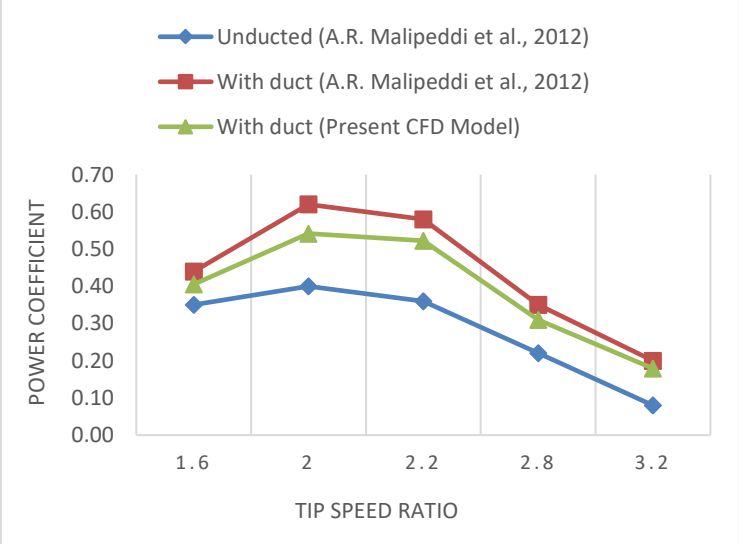

Fig. 2. Validation of the present and previous results

4.2 Torque Output and Torque Coefficient Analysis

The performance of the water turbine is often governed by aerodynamic parameters such as torque and torque coefficient, especially in a hydro turbine. As a result, Figure 3 and 4 show the

outputs of the numerical simulation torque and torque coefficient achieved by the NACA 663-018 airfoil using CFD simulations with a constant inlet velocity of 1.1 m/s. As seen in Figure 3, the trend line is rising from tip speed ratio (TSR) = 1.6 to tip speed ratio (TSR) = 2, which is where the maximum torque value is located. Beyond the value of 2 TSR, as the TSR is increasing, the torque values is decreasing until it reached the TSR of 2.8, where the lowest torque value lies. Moreover, Figure 4 shows that the torque coefficient value increased from tip speed ratio (TSR) of 1.6 to the TSR of 2 when it achieved its maximum value. Then, the trend line change and continue to decrease until it reached the lowest value of torque coefficient which is located at the TSR of 3.2. nonetheless, the torque coefficient value may experience some negative values before turning back to positive values if the TSR is continuously growing. This may be the result of flow separations that happen when the water passes through and an increase in blade pressure that also produces a static stall.

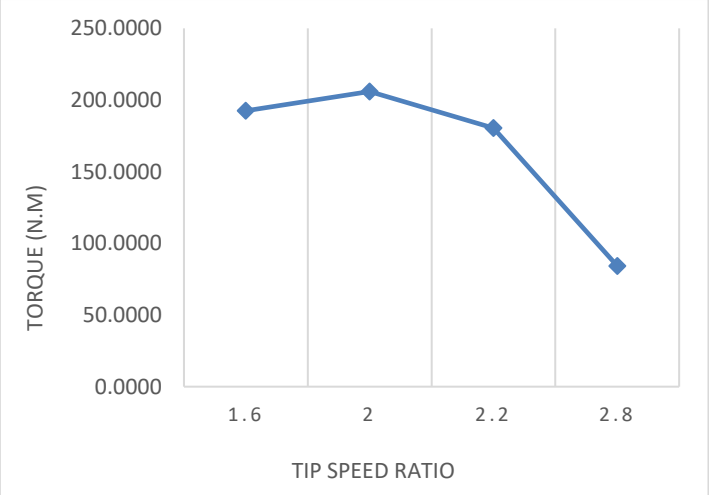

Fig. 3. Torque output against TSR

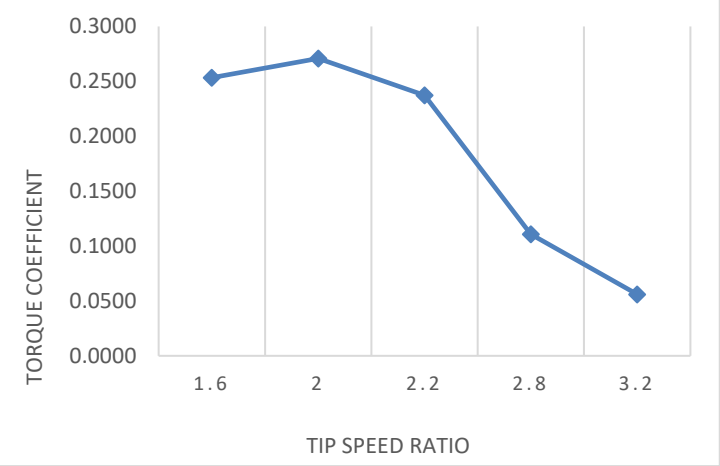

Fig. 4. Torque output against TSR

4.3 Power Output and Power Coefficient Analysis

The ratio of the power extracted by the hydro turbine to the energy present in the water stream is known as the power coefficient. Therefore, the efficiency of a turbine can be derived by obtaining the values of the power coefficient. As the torque values are obtained from the 2D simulations in CFD, the power and power coefficients (Cp) may be calculated using equation (Eq. (6) and Eq. (7))

and presented in a graph against tip speed ratio (TSR) as shown in Figure 5 and Figure 6. Moreover, Figure 5 shows the numerical simulation results of the power output against the TSR. From the graph, it can be observed that the power output values increase as the TSR is increasing reaching the peak at the TSR of 2 and then it starts to decrease reaching the lowest power value which is at TSR of 2.8. Therefore, it can be deduced that the power output is at its highest when the TSR is 2. Furthermore, Figure 6 shows the simulation results of the power coefficient against the TSR. From the graph, it can be observed that the trend line is similar to the power output graph shown in Figure 5, as expected. The power coefficient gradually increases starting from the lowest TSR of 1.6 and plummets after the TSR reaches 2 and finally reached the lowest value of power coefficient which is at TSR of 3.2. As such, it is known that the higher the value of the power coefficient, the better the efficiency of a turbine. Hence, it can be concluded that the turbine works most efficiently at TSR of 2.

In addition, to analyse the impact of the pressure and velocity, the pressure contours and velocity contours of the NACA 663-018 airfoil rotor at optimal TSR of 2 are used. These contours are illustrated in Figure 7, 8 and 9. Figure 7 depicts the pressure contours, which show that larger pressures occur towards the leading edge of the blade. This demonstrated that stagnation occurs at the blade's leading edges, where the velocity is substantially lower before flowing into the upper and lower bodies of the blades. The pressure on the bottom surface of the airfoil was then larger than the pressure in the entering flow stream. As a result, trust was built upstream of the airfoil. This pressure differential across the blades primarily determines the driving power used to generate torque to operate the turbine.

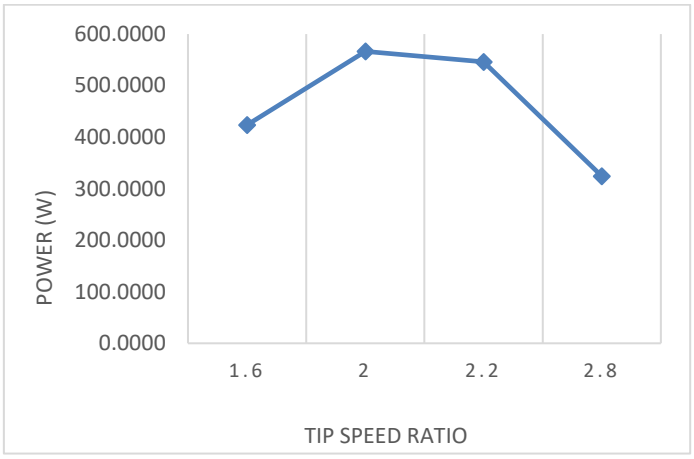

Fig. 5. Power output against TSR

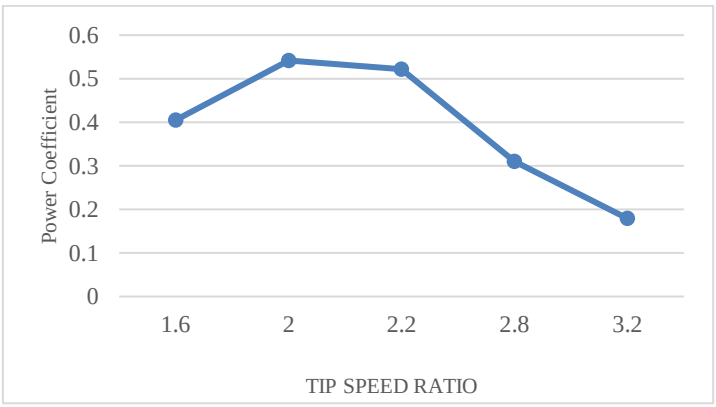

Fig. 6. Power coefficient output against TSR

Moreover, Figure 8 illustrates the velocity contours around the NACA66$_3$-018 airfoil rotor. Reasonably, when the incoming water comes in contact with the blades, the rotor will start to spin and consequently forcing the water around the rotor to move in a circular pattern as well. This circular movement of the water around the rotor somehow affects the performance of the rotor due to the velocity of the incoming water on returning blades being reduced and consequently generating resistance between the blade surface and the incoming water. By analysing the velocity contour, it can be seen that the velocity at the leading edge of all the blades is lower which supported the occurrence of stagnation that was mentioned previously. It is also notable that a small wind vortex had built up inside the rotor given that relatively low velocity can be observed inside the rotor. Moreover, the figure shows that the velocity of the water increases until it reached the throat of the duct where the flow is converging. It is known that the stream velocity in the duct is going to be highest at the narrowest position of the duct as a result of the continuity equation.

Furthermore, as seen in Figure 9, flow separation occurs at the outer side of the duct and also downstream of the duct. It is known that after passing through a broadening passage, such as the downstream of the duct, or the thickest portion of a streamlined body, such as the outer side of the duct, flow separation always happens in a flow that is reducing in velocity but increasing in pressure.

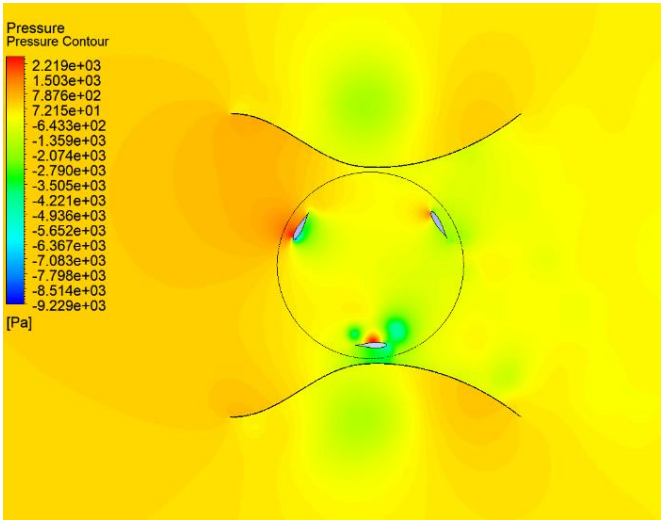

Fig. 7. Dynamic pressure contour of the bionic blade at 10 ms^{-1} inlet velocity

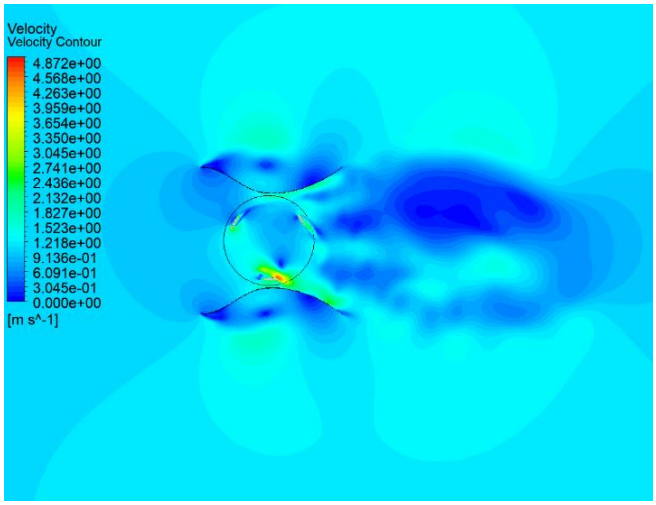

Fig. 8. Velocity contour of the bionic blade under 10 ms^{-1} inlet velocity

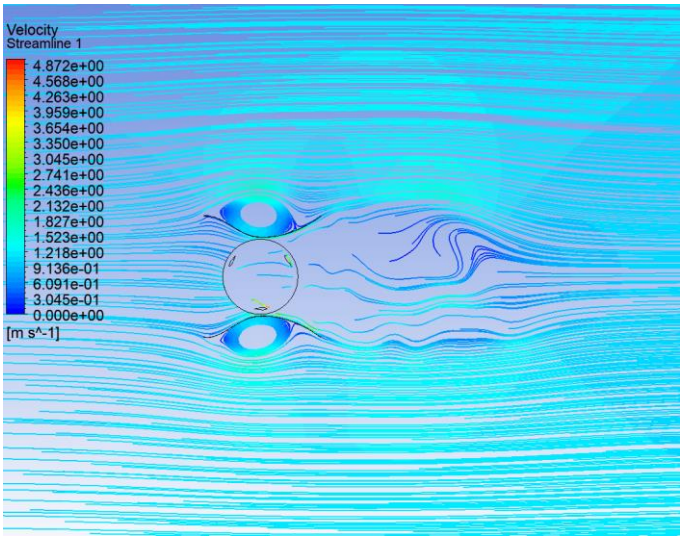

Fig. 9. Streamline of the bionic blade under the inlet velocity of 10 ms^{-1}

5. Conclusions

In this study, a 2D numerical simulation study utilizing computational fluid dynamics (CFD) was carried out to investigate the impact of the duct geometry on the performance of the Darrieus turbine with NACA 66_3-018 airfoil profile. The investigation was carried out using the software ANSYS Fluent and the simulation used a K-ω Shear Stress Transport (SST) turbulence model. The performance evaluation of the NACA 66_3-018 airfoil model is conducted by using various rotational speeds while keeping the incoming water velocity of 1.1 m/s. The simulation results show that the power coefficient and torque coefficient were found to increase with the TSR with the highest efficiency at the TSR of 2 and then decrease. A similar conclusion was drawn in terms of power and torque output. Moreover, according to the results, the turbine is most effective when the tip speed ratio (TSR) is 2, where the power coefficient and torque coefficient are respectively 54% and 27%.

Acknowledgement

The authors would like to acknowledge the financial support provided by the Universiti Tun Hussein Onn Malaysia through the H919 grant.

References

[1] International Energy Agency, "Access to electricity – SDG7: Data and Projections – Analysis - IEA." *SDG7: Data and Projections*, 2021.

[2] Didane, Djamal Hissein, Mohd Fadhli Zulkafli, Sofian Mohd, Mohd Faizal Mohideen Batcha, and Amir Khalid. "Development and Performance Investigation of a Unique Dual-rotor Savonius-type Counter-rotating Wind Turbine." *International Journal of Integrated Engineering* 13, no. 6 (2021): 89-98.

[3] Didane, Djamal Hissein, Muhammad Nur Arham Bajuri, Bukhari Manshoor, and Mahamat Issa Boukhari. "Performance Investigation of Vertical Axis Wind Turbine with Savonius Rotor using Computational Fluid Dynamics (CFD)." *CFD Letters* 14, no. 8 (2022): 116-124. https://doi.org/10.37934/cfdl.14.8.116124

[4] Ahuja, Dilip, and Marika Tatsutani. "Sustainable energy for developing countries." *SAPI EN. S. Surveys and Perspectives Integrating Environment and Society* 2.1 (2009).

[5] Nielsen, Torbjorn K., Cuthbert Z. Kimambo, and Chiyembekezo S. Kaunda. "Hydropower in the Context of Sustainable Energy Supply: A Review of Technologies and Challenges." (2012). https://doi.org/10.5402/2012/730631

[6] Weisensee, Patricia, and Magdi Ragheb. "Integrated wind and solar qattara depression project with pumped storage as part of desertec." *Proceedings of the RETBE* 12 (2012).

[7] Khan, M. J., G. Bhuyan, M. T. Iqbal, and J. E. Quaicoe. "Hydrokinetic energy conversion systems and assessment of horizontal and vertical axis turbines for river and tidal applications: A technology status review." *Applied energy* 86, no. 10 (2009): 1823-1835. https://doi.org/10.1016/j.apenergy.2009.02.017

[8] Loutun, Mark Jason Thomas, Djamal Hissein Didane, Mohd Faizal Mohideen Batcha, Kamil Abdullah, Mas Fawzi Mohd Ali, Akmal Nizam Mohammed, and Lukmon Owolabi Afolabi. "2D CFD Simulation Study on the Performance of Various NACA Airfoils." *CFD Letters* 13, no. 4 (2021): 38-50. https://doi.org/10.37934/cfdl.13.4.3850

[9] Gorlov, Alexander M. "The helical turbine: A new idea for low-head hydro." *Hydro Review* 14, no. 5 (1995).

[10] Didane, Djamal Hissein, Muhammad Amir Zafran Saipul Anuar, Mohd Faizal Mohideen Batcha, Kamil Abdullah, Mas Fawzi Mohd Ali, and Akmal Nizam Mohammed. "Simulation study on the performance of a counter-rotating savonius vertical axis wind turbine." *CFD Letters* 12, no. 4 (2020): 1-11. https://doi.org/10.37934/cfdl.12.4.111

[11] Didane, Djamal Hissein, Nurhayati Rosly, Mohd Fadhli Zulkafli, and Syariful Syafiq Shamsudin. "Performance evaluation of a novel vertical axis wind turbine with coaxial contra-rotating concept." *Renewable Energy* 115 (2018): 353-361. https://doi.org/10.1016/j.renene.2017.08.070

[12] Didane, Djamal Hissein, Nurhayati Rosly, Mohd Fadhli Zulkafli, and Syariful Syafiq Shamsudin. "Numerical investigation of a novel contra-rotating vertical axis wind turbine." *Sustainable Energy Technologies and Assessments* 31 (2019): 43-53. https://doi.org/10.1016/j.seta.2018.11.006

[13] Didane, D. H., S. M. Maksud, M. F. Zulkafli, N. Rosly, S. S. Shamsudin, and A. Khalid. "Experimental Study on the Performance of a Savonius-Darrius Counter-Rotating Vertical Axis Wind Turbine." In *IOP Conference Series: Earth and Environmental Science*, vol. 268, no. 1, p. 012060. IOP Publishing, 2019. https://doi.org/10.1088/1755-1315/268/1/012060

[14] Didane, Djamal Hissein, Siti Masyafikah Maksud, Mohd Fadhli Zulkafli, Nurhayati Rosly, Syariful Syafiq Shamsudin, and Amir Khalid. "Performance investigation of a small Savonius-Darrius counter-rotating vertical-axis wind turbine." *International Journal of Energy Research* 44, no. 12 (2020): 9309-9316. https://doi.org/10.1002/er.4874

[15] Didane, D. H., Sofian Mohd, Z. Subari, Nurhayati Rosly, MF Abdul Ghafir, and MF Mohd Masrom. "An aerodynamic performance analysis of a perforated wind turbine blade." In *IOP Conference Series: Materials Science and Engineering*, vol. 160, no. 1, p. 012039. IOP Publishing, 2016. https://doi.org/10.1088/1757-899X/160/1/012039

[16] Alquraishi, Balasem Abdulameer, Nor Zelawati Asmuin, Sofian Mohd, Wisam A. Abd Al-Wahid, and Akmal Nizam Mohammed. "Review on diffuser augmented wind turbine (dawt)." *International Journal of Integrated Engineering* 11, no. 1 (2019).

[17] Al-Ghriybah, Mohanad, Mohd Fadhli Zulkafli, Djamal Hissein Didane, and Sofian Mohd. "The effect of inner blade position on the performance of the Savonius rotor." *Sustainable Energy Technologies and Assessments* 36 (2019): 100534. https://doi.org/10.1016/j.seta.2019.100534

[18] Al-Ghriybah, Mohanad, Mohd Fadhli Zulkafli, Djamal Hissein Didane, and Sofian Mohd. "Performance of the Savonius Wind Rotor with Two Inner Blades at Low Tip Speed Ratio." *CFD Letters* 12, no. 3 (2020): 11-21. https://doi.org/10.37934/cfdl.12.3.1121

[19] Halmy, Muhammad Syahmy Mohd, Djamal Hissein Didane, Lukmon Owolabi Afolabi, and Sami Al-Alimi. "Computational Fluid Dynamics (CFD) Study on the Effect of the Number of Blades on the Performance of Double-Stage Savonius Rotor." *Cfd Letters* 13, no. 4 (2021): 1-10. https://doi.org/10.37934/cfdl.13.4.110

[20] Menter, Florian R. "Two-equation eddy-viscosity turbulence models for engineering applications." *AIAA journal* 32, no. 8 (1994): 1598-1605. https://doi.org/10.2514/3.12149

[21] Malipeddi, A. R., and D. Chatterjee. "Influence of duct geometry on the performance of Darrieus hydroturbine." *Renewable Energy* 43 (2012): 292-300. https://doi.org/10.1016/j.renene.2011.12.008